Normal-mode decomposition for the optical response of cylinder clusters

A. J. Reuben and G. B. Smith
Department of Applied Physics, University of Technology, Sydney, P.O. Box 123, Broadway, New South Wales 2007, Australia
(Received 18 August 1997)

We present a powerful technique that generates the complete normal-mode representation for the two-dimensional quasistatic response of *any* finite cluster of nonintersecting cylinders. We initially study two particular structures, a rectangular and then a triangular arrangement of cylinders. In each case a superposition technique involving two coordinate frames is used to obtain eigenfunction expansions for the induced electrostatic potential. Imposition of boundary conditions at each cylinder surface generates a system of equations for the expansion coefficients in which optical and geometric factors can be trivially separated. This produces a so-called structure matrix whose eigenvalues determine the resonance positions for the total response. The weights for these uncoupled and independent resonances are also readily calculated. Predicted results for the two chosen arrangements are then given. We conclude by showing how the technique is extended to cover general finite clusters of nonintersecting cylinders. [S1063-651X(98)06907-4]

PACS number(s): 41.20.Cv, 78.20.Bh, 78.20.Ci, 02.30.Em

I. INTRODUCTION

Interest in the optical and electrical transport properties of composite materials has a long history [1]. The standard averaging methods for random arrays such as the Maxwell-Garnet [2], Lorentz-Lorenz [3,4], Bruggeman, and Clausius-Mossotti formulations are essentially dipole theories with limited applicability. Interest has come to center on the question of the importance of long-range interactions for both ordered and disordered particulate arrays as well as on the effect of a close approach between individual particles. One way of gaining insight into such questions is to consider finite clusters. In particular, one would like to understand how a given geometric arrangement of particles determines the polarizability. In general the most accessible problems seem to be those involving ordered arrays of infinite extent or finite clusters that rarely involve more than two particles. The generally *ad hoc* methods used in these instances have tended to employ imaging or conformal mapping methods. In all but a handful of these approaches major disadvantages tend to surface. Moreover, the very general formalisms that have appeared are rarely of practical use in concrete situations. Only in a few have the individual resonances for the polarization been determined together with their corresponding strengths [5,6]. In this work we solve this problem for any finite cluster of circular cylinders.

Although for the general dynamic problem there is as yet no general theory relating the optical properties of a composite to its geometry, in the quasistatic realm the closest thing to this is the Bergman spectral representation [7]. In this formulation the average dielectric function (per unit area) of a two-component system of relative dielectric ϵ has the representation

$$\langle \chi \rangle = \sum_n \frac{g_n}{\chi^{-1} + L_n}, \quad \chi = \epsilon - 1, \tag{1}$$

where the spectral weights g_n and depolarization factors L_n satisfy

$$g_n \geqslant 0, \quad 0 \leqslant L_n \leqslant 1, \tag{2}$$

$$\sum_n g_n = 1. \tag{3}$$

In Secs. III and IV a technique will be applied to both rectangular and triangular clusters of cylinders that yields complete normal-mode Bergman decompositions in each case. Moreover, there are no restrictions on the dielectric constants of either host or inclusion. Hence it is expected that this approach, which will be extended to general clusters in Sec. VI, should find wide application.

The technique used here always leads to an explicit Bergman decomposition for the polarizability. This is because the system of equations defining the coefficients in the series expansion for the external field takes the following form [5]:

$$(\nu \boldsymbol{I} + \boldsymbol{S}) \cdot \mathbf{X} = \mathbf{Y}, \tag{4}$$

where

$$\nu = -1 - 2\chi^{-1} \tag{5}$$

and $\mathbf{X}$ is the sought-after vector of potential coefficients x_i, $\mathbf{Y}$ a vector of constants y_i, $\boldsymbol{I}$ the unit matrix, and $\boldsymbol{S}$ the so-called *structure matrix*, which only depends on the geometric arrangement of the cylinders in the cluster.

Diagonalizing the structure matrix $\boldsymbol{S}$ leads to

$$\boldsymbol{U}^{-1} \cdot \boldsymbol{S} \cdot \boldsymbol{U} = \boldsymbol{T}, \tag{6}$$

where $\boldsymbol{U}$ and its inverse are matrices of elements u_{ij} and $\overline{u}_{ij}$, respectively, and $\boldsymbol{T}$ is the diagonal matrix whose elements are $\delta_{ij} t_j$, the t_i being the eigenvalues of $\boldsymbol{S}$. Consequently Eq. (4) becomes

$$(\nu \boldsymbol{I} + \boldsymbol{T}) \cdot \mathbf{X}' = \mathbf{Y}', \tag{7}$$

where

$$\begin{Bmatrix} \mathbf{X}' \\ \mathbf{Y}' \end{Bmatrix} = \boldsymbol{U}^{-1} \cdot \begin{Bmatrix} \mathbf{X} \\ \mathbf{Y} \end{Bmatrix}. \tag{8}$$

Solving Eq. (7) for $\mathbf{X}'$ and then applying Eq. (8) leads to

$$x_i = \sum_{j,k} \frac{u_{ik}\overline{u}_{kj} y_j}{\nu + t_k}. \tag{9}$$

The polarizability will be found by determining the $1/r$ coefficient in the far-field expansion of the induced external potential. As will be shown in the following sections, this will turn out to be a linear combination of the potential coefficients. Hence for some sequence of positive constants f_i we will obtain

$$\langle \chi \rangle = \sum_n \frac{g_n'}{\nu + t_n}, \tag{10}$$

where

$$g_n' = \sum_{i,j} f_i u_{in} \overline{u}_{nj} y_j. \tag{11}$$

We thus obtain the full Bergman representation (1) with spectral weights and depolarization factors given by

$$g_n = \tfrac{1}{2} g_n', \quad L_n = \tfrac{1}{2}(1 - t_n). \tag{12}$$

All that then remains to be done is to obtain the key equation (4), determine the eigenvalues of $\boldsymbol{S}$, and then insert the appropriate constants f_i.

We shall exemplify the technique by applying it to a rectangular and then to a triangular cluster of identical cylinders. We consider the infrared limit for which an electrostatic approach to the problem of small particles in a constant uniform electric field is sufficient. In such a limit the wavelength of the external field is assumed to be much greater than the particle diameters and the distances separating the particles. In this situation the approach outlined above is applicable and yields a seminumerical solution for any desired number of resonance positions and corresponding weights. In both the rectangular and triangular clusters the matrix equation (4) representing the truncated system of equations for the induced potential coefficients will be obtained. In Sec. V we will analyze the eigenvalue spectra and the corresponding sets of weights for various possible cylinder arrangements in these two cases. We now proceed to introduce the basic background concepts.

II. METHODOLOGY

We shall build on recently developed techniques that have all given insights into the responses of either a pair or an infinite array of cylindrical inclusions [8–11]. As in these earlier studies, the procedure adopted here can be most lucidly presented by working throughout in terms of appropriate complex variables. This also provides the possibility of making a more concise presentation of the mathematical machinery. Moreover, by obtaining the potential induced for any one given field direction as the real part of a complex series expansion, all other information is also found. The corresponding imaginary part of the induced potential will generate the flux lines for this direction, while the replacement of dielectric constants with their reciprocals will automatically produce the potential for the orthogonal direction (Keller's theorem [12]). Together these two solutions can then provide polarizations for arbitrary field directions simply by combining components of each in varying proportions.

The key to the following approach is to note that the induced electrostatic potentials are harmonic functions that vanish at infinity and hence that *the sum of any two such functions is again a valid outer potential*. We thus partition the whole cluster into a set of subclusters and define the ''local'' coordinate frame for a given subcluster to be a frame that contains a coordinate contour representing the boundary (or boundaries) of the cylinder(s) in the given subcluster. We write down inner and outer potential expansions for each subcluster in their respective local coordinates. Each subcluster will thus contribute its own local external potential and the total induced potential will be the sum of these. All that remains to be done is to satisfy the appropriate boundary conditions at each cylinder surface. The sets of coefficients are found from the system of equations (4) generated by successive imposition of the boundary conditions within each subcluster. The crucial feature of this approach is the ability to reexpand each local eigenfunction expansion in terms of the eigenfunctions in every other local variable in such a way that the resulting series converge on each cylinder boundary.

We now consider an applied field of unit strength acting along the horizontal axis. At all cylinder boundaries the following matching conditions must be satisfied by the outer ($\phi^{(1)}$), inner ($\phi^{(2)}$), and applied ($\phi^{(\mathrm{app})}$) potentials:

$$\phi^{(\mathrm{app})} + \phi^{(1)} = \phi^{(2)}, \tag{13}$$

$$\frac{\partial \phi^{(\mathrm{app})}}{\partial n} + \frac{\partial \phi^{(1)}}{\partial n} = \epsilon \frac{\partial \phi^{(2)}}{\partial n}. \tag{14}$$

Our approach will be to use the above-mentioned superposition technique with subclusters containing either a single cylinder or a pair of cylinders. The local coordinate frames corresponding to these subclusters will be the polar and bicylindrical frames, respectively [10]. The Laplace equation in such frames is unchanged and so its solutions will be the usual combinations of hyperbolic and trigonometric functions in the transformed variables [13]. The bicylindrical coordinate frame is illustrated in Fig. 1.

III. RECTANGULAR CLUSTER

We now consider the rectangular array consisting of the four identical unit cylinders shown in Fig. 2. The horizontal and vertical distances separating the cylinder centers are given by $2d$ and $2b$, respectively. The external field direction will be along the horizontal (x) axis and so we introduce the complex variable $z = x + iy$ and express the applied potential everywhere as the real part of

$$\phi^{(\mathrm{app})} = z. \tag{15}$$

We shall consider the response for this geometry as resulting from the interaction between the upper and lower cylinder

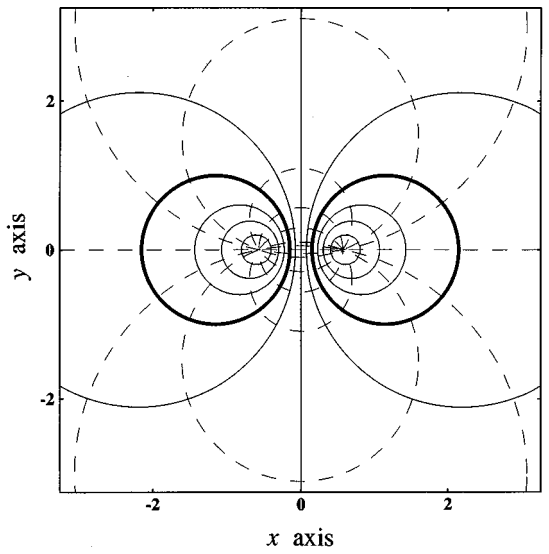

FIG. 1. The bicylindrical coordinate frame showing contours of constant u (solid) and constant v (dashed). The boundaries of the unit cylinders centered on the x axis at $d=\pm 1.1$ are shown in bold.

pairs. The local coordinate system for the upper pair will be the transformed variable w_+ where

$$w_+ = u_+ + iv_+ = \frac{1}{2a}\ln\frac{z-ib+a}{z-ib-a}, \tag{16}$$

which is just the bicylindrical frame shifted upwards from the x axis by an amount b. Analogously the corresponding local coordinate system for the lower pair will be generated by the transformation

$$w_- = u_- + iv_- = \frac{1}{2a}\ln\frac{z+ib+a}{z+ib-a}. \tag{17}$$

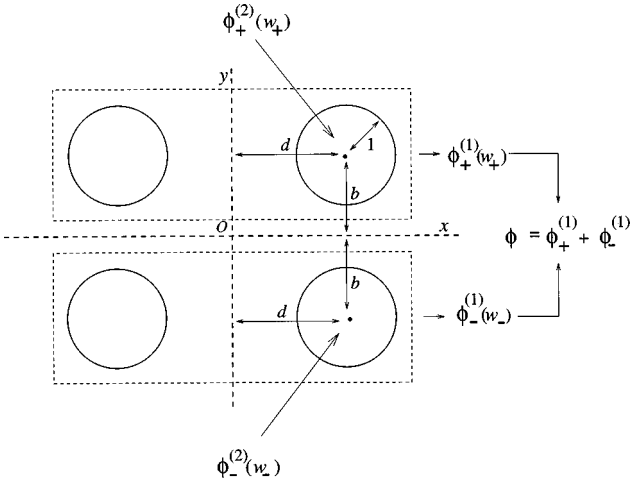

FIG. 2. A rectangular arrangement of circular unit cylinders. The cylinders are centered at the points $(\pm d, \pm b)$. The cluster is partitioned into an upper and lower pair (each shown boxed), which have respective bicylindrical coordinate frames, $w_\pm$, assigned to them. The corresponding inner ($\phi_\pm^{(2)}$) and outer ($\phi_\pm^{(1)}$) potentials are indicated. The total induced outer potential, ϕ, is the sum of the individual outer potential contributions.

For cylinder pairs with center-to-center separation of $2d$ the equation defining the boundary of the right-hand unit cylinder will be given by $u=u_1$ where [10]

$$a=\sqrt{d^2-1}, \quad u_1=\frac{1}{2a}\ln(a+\sqrt{1+a^2}). \tag{18}$$

The total outer potential ϕ will be taken as the sum of the outer potentials around the upper and lower pairs, $\phi_+^{(1)}$ and $\phi_-^{(1)}$, respectively. Moreover, these potentials will each be eigenfunction expansions in terms of their respective local variables, $w_\pm$. Due to the presence of the other pair, the individual outer potentials, $\phi_\pm^{(1)}$, will not be symmetric about their respective horizontal axes (the lines $y=\pm b$). These local outer potentials must therefore contain terms in both $\sin 2anv$ and $\cos 2anv$ and will thus be given by the real parts of the following expressions:

$$\phi_\pm^{(1)} = \sum_{n=1}^{\infty} A_n^\pm \sinh 2anw_\pm - iB_n^\pm \cosh 2anw_\pm . \tag{19}$$

The same symmetry considerations generate potentials valid inside the upper and lower right-hand cylinders. These will be the real parts of

$$\phi_\pm^{(2)} = \sum_{n=1}^{\infty} (C_n^\pm - iD_n^\pm) e^{-2anw_\pm}. \tag{20}$$

The total induced (outer) potential will then be given by the real part of

$$\phi = \phi_+^{(1)} + \phi_-^{(1)}. \tag{21}$$

There are thus eight coefficients in all. However, since the functions $\cosh 2anw_\pm$ are even in $z\pm ib$, only the coefficients $A_n^\pm$ of the functions $\sinh 2anw_\pm$ need to be determined explicitly in order to find the polarizability. The magnitudes of the coefficients $B_n^\pm$ reflect the degree of interaction between the pairs and vanish as $b\to\infty$. There are four boundary conditions, two on the upper cylinder pair and two on the lower pair. Each of these equations will involve series in both $\cos 2anv_\pm$ and $\sin 2anv_\pm$. These can thus in turn be separated into two equations and so the total number of equations becomes eight, as required.

The procedure for now building the system of equations which defines the coefficients is successively to match the potential ϕ and its normal derivative $\partial\phi/\partial n$ with the appropriate internal potentials across the upper and lower cylinder pair boundaries. In the former case everything is to be expressed in terms of the upper variables, w_+, and in the latter, in terms of the lower variables, w_-. Due to the symmetry of the problem about the horizontal axis, each upper coefficient will mirror the corresponding lower one. In fact, once the matching is performed on the upper pair, the corresponding equations for the lower matching can be found by merely replacing b with $-b$ everywhere. It will be found convenient to use the following definitions:

$$\rho=\sqrt{1+a^2/b^2}, \quad \varpi=\tan^{-1}\frac{a}{b}. \tag{22}$$

So, in matching on the upper pair, the variable in which we work is w_+. The eigenfunction expansion for the applied potential z is found from Eq. (16). To within a constant factor it is given by [10]

$$\phi^{(\mathrm{app})}=2a\sum_{n=1}^{\infty} e^{-2anw_+}. \tag{23}$$

We must now express the exponentials in w_- in terms of the eigenfunctions e^{-2akw_+} in Eq. (23). We have from Eqs. (16) and (17) that

$$e^{2anw_-}=\rho^n e^{-in\varpi}\left(\frac{1-s/\rho^2}{1-s}\right)^n, \tag{24}$$

where

$$s=\left(1+\frac{a}{b}\,i\right)e^{-2aw_+}. \tag{25}$$

We would like to be able to expand the expression (24) in the appropriate powers of s such that the result converges along the upper right-hand cylinder. Now it turns out that the expression in brackets in Eq. (24) is effectively the generating function for the so-called Meixner polynomials [14]. For $|\xi|<\min(1,|c|)$, we have [14,15]

$$\left(\frac{1-\xi/c}{1-\xi}\right)^n=\sum_{k=0}^{\infty} m_{n,k}(c)\,\xi^k, \tag{26}$$

where

$$m_{n,k}(c)=n\Gamma(k+1)\left(1-\frac{1}{c}\right)F_{2,1}\left(1-k,1-n;2;1-\frac{1}{c}\right), \tag{27}$$

with the $F_{2,1}(a,b;c;z)$ denoting the Gaussian hypergeometric functions [15]. Applying Eq. (26) to both Eq. (24) and its reciprocal produces

$$e^{\pm 2anw_-}=\pm n\left(1-\frac{1}{\rho^2}\right)\rho^{\pm n}e^{\mp in\varpi}\times\sum_{k=0}^{\infty} F_{2,1}\left(1-k,1\mp n;2;1-\frac{1}{\rho^2}\right)\rho^k e^{ik\varpi}e^{-2akw_+}. \tag{28}$$

This immediately leads to the following expansions for the hyperbolic functions in w_-:

$$\begin{Bmatrix}\sinh 2anw_-\\ \cosh 2anw_-\end{Bmatrix}=\sum_{k=0}^{\infty}(G_{n,k}^{\pm,c}+iG_{n,k}^{\pm,s})e^{-2akw_+}, \tag{29}$$

where

$$G_{n,k}^{\pm,\{{}^{c}_{s}\}}=G_{n,k}^{\pm,\{{}^{c}_{s}\}}(\rho,\varpi)=\frac{n}{2}\left(1-\frac{1}{\rho^2}\right)\left\{\rho^{k+n}F_{2,1}\left(1-k,1-n;2;1-\frac{1}{\rho^2}\right)\begin{Bmatrix}\cos\\ \sin\end{Bmatrix}((k-n)\varpi)\pm\rho^{k-n}F_{2,1}\left(1-k,1+n;2;1-\frac{1}{\rho^2}\right)\times\begin{Bmatrix}\cos\\ \sin\end{Bmatrix}((k+n)\varpi)\right\}. \tag{30}$$

The real parts of the hyperbolic functions (29) will thus contain contributions from both $\sin 2akv_+$ and $\cos 2akv_+$. In fact, the complex contributions in the coefficients embody the interaction between the upper and lower pairs and as $b\to\infty$ $(\varpi\to 0)$ the terms $G_{n,k}^{\pm,s}$ in Eq. (29) will tend to zero. The proof that the expansions (29) converge on the upper right-hand unit cylinder appears in Appendix A.

We can now write down the boundary condition (13) along the upper right-hand cylinder $(u_+=u_1)$ using Eqs. (19) and (20) for $\phi_+^{(1)}$ and $\phi_+^{(2)}$, respectively, Eqs. (19) and (29) for $\phi_-^{(1)}$, and Eq. (23) for $\phi^{(\mathrm{app})}$. By taking real parts in the resulting equation we will obtain two sets of terms, those multiplying $\sin 2akv_+$ and those multiplying $\cos 2akv_+$. Since these are independent eigenfunctions, we can drop the outer summation and split the two sets into two separate equations. The second boundary condition, Eq. (14), effected here by taking derivatives with respect to u_+, will similarly lead to another two equations. Combining these four equations to eliminate C_n^+ and D_n^+ then leads to

$$A_k^+(\nu+\mu^k)-\sum_{n=1}^{\infty}\tilde{G}_{n,k}^{+,c}A_n^--\sum_{n=1}^{\infty}\tilde{G}_{n,k}^{-,s}B_n^-=2a\mu^k, \tag{31}$$

$$B_k^+(\nu+\mu^k)-\sum_{n=1}^{\infty}\tilde{G}_{n,k}^{+,s}A_n^-+\sum_{n=1}^{\infty}\tilde{G}_{n,k}^{-,c}B_n^-=0, \tag{32}$$

where

$$\tilde{G}_{n,k}=\mu^k G_{n,k}. \tag{33}$$

To obtain the two analogous equations on the lower pair of cylinders $(u_-=u_1)$ we everywhere replace b with $-b$. This generates a pair of equations analogous to Eqs. (31) and (32) for the lower cylinder pair, which, when compared with Eqs. (31) and (32), immediately implies

$$A_n^+ = A_n = A_n^- , \quad B_n^+ = B_n = -B_n^- . \tag{34}$$

Writing the system Eqs. (31)–(34) in matrix form leads to the truncated analog of Eq. (4). Using the subscript m to denote truncation to order m, we obtain the following for the coefficients A_k and B_k:

$$(\nu \boldsymbol{I}_{2m} + \boldsymbol{S}_m^{(\mathrm{rect})}) \cdot \mathbf{X}_m = \mathbf{Y}_m , \tag{35}$$

where $\boldsymbol{I}_m$ denotes the $m \times m$ unit matrix,

$$\mathbf{X}_m = \begin{pmatrix} \mathbf{A}_m \\ \cdots \\ \mathbf{B}_m \end{pmatrix}, \quad \mathbf{Y}_m = 2 \begin{pmatrix} \mathbf{K}_m \\ \cdots \\ \mathbf{O}_m \end{pmatrix} \tag{36}$$

and the structure matrix is

$$\boldsymbol{S}_m^{(\mathrm{rect})} = \begin{pmatrix} \boldsymbol{E}_m - \tilde{\boldsymbol{G}}_m^{+,c} & \vdots & \tilde{\boldsymbol{G}}_m^{-,s} \\ \cdots & \vdots & \cdots \\ -\tilde{\boldsymbol{G}}_m^{+,s} & \vdots & \boldsymbol{E}_m - \tilde{\boldsymbol{G}}_m^{-,c} \end{pmatrix} \tag{37}$$

where

$$\boldsymbol{E}_m = \begin{pmatrix} \mu & 0 & \cdots & 0 \\ 0 & \mu^2 & \ddots & \vdots \\ \vdots & \ddots & \ddots & 0 \\ 0 & \cdots & 0 & \mu^m \end{pmatrix}, \quad \mathbf{K}_m = 2a \begin{pmatrix} \mu \\ \mu^2 \\ \vdots \\ \mu^m \end{pmatrix}, \tag{38}$$

with $\mathbf{A}_m$ and $\mathbf{B}_m$ denoting the vectors of coefficients A_i and B_i, respectively, the $\tilde{\boldsymbol{G}}^{\pm,p}$ $(p=c,s)$ being matrices of elements $\tilde{G}_{i,j}^{\pm,p}$ and $\mathbf{O}_m$ the null column vector.

The total polarizability of the rectangular cluster will be made up of the sum of the upper and lower cylinder pair contributions and will only come from the $\sinh 2anw$ terms in Eq. (19). So, using Eq. (34), we obtain [10]

$$\langle \chi \rangle_{\mathrm{rect}} = 2a \sum_{n=1}^{\infty} n A_n . \tag{39}$$

The spectral decomposition for the rectangular cluster is thus Eq. (1) with

$$g_n = 4a^2 \sum_{i=1}^{m} \sum_{j=1}^{m} i \mu^j u_{in} \overline{u}_{nj}, \quad L_n = \tfrac{1}{2}(1 - t_n), \tag{40}$$

for $n = 1,\ldots,2m$, where the u_{ij} and $\overline{u}_{ij}$ are the elements of the matrices $\boldsymbol{U}$ and $\boldsymbol{U}$ which diagonalize the structure matrix $\boldsymbol{S}_m^{(\mathrm{rect})}$ and the t_n are the eigenvalues of this matrix.

IV. TRIANGULAR CLUSTER

For the triangular arrangement of unit cylinders shown in Fig. 3 we shall again consider an externally applied field acting along the x axis. This time we shall use a polar frame for the upper cylinder and a bicylindrical one for the lower pair. For the upper cylinder centered at $z = ib$ we have

$$w_+ = \ln(z - ib) = u_+ + i v_+ = \ln r + i\theta, \tag{41}$$

while for the lower pair aligned along the x axis at the points $z = \pm d$ we have

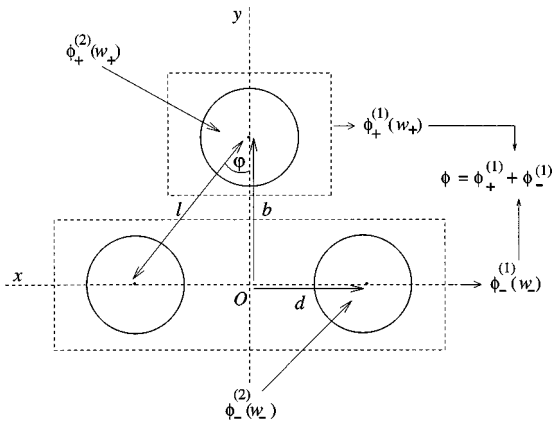

FIG. 3. A triangular arrangement of circular unit cylinders. The upper cylinder is centered on the y axis at the point $(0,b)$ while the lower pair of cylinders is centered at the points $(\pm d,0)$ on the x axis. The cluster here is partitioned into two subclusters (each shown boxed) with a polar frame, w_+, used for the upper cylinder, and a bicylindrical frame, w_-, used for the cylinder pair lying on the x axis. Inner $(\phi_\pm^{(2)})$ and outer $(\phi_\pm^{(1)})$ potentials are indicated. The total induced outer potential, ϕ, is the sum of the individual outer potential contributions.

$$w_- = \frac{1}{2a} \ln\left(\frac{z+a}{z-a}\right) = u_- + i v_- . \tag{42}$$

The boundary of the upper unit cylinder is given by $u_+ = 0$ $(r = 1)$ while for the lower right-hand cylinder we again have Eq. (18).

Proceeding as for the rectangular arrangement, we define the two local outer potentials. Each will possess left-right symmetry only and so as before there will be two coefficients in each eigenfunction expansion. In particular, the upper expansions will contain terms in both $\sin k\theta$ and $\cos k\theta$. For the upper cylinder the appropriate form is thus the real part of

$$\phi_+^{(1)} = \sum_{n=1}^{\infty} A_n^+ e^{-(2n-1)w_+} - i B_n^+ e^{-2nw_+}, \tag{43}$$

while for the lower pair it is, as before, the real part of

$$\phi_-^{(1)} = \sum_{n=1}^{\infty} A_n^- \sinh 2anw_- - i B_n^- \cosh 2anw_- , \tag{44}$$

and so the total induced potential for the triangular arrangement will be the real part of

$$\phi = \phi_+^{(1)} + \phi_-^{(1)} . \tag{45}$$

We now write down the complex potentials inside the upper cylinder,

$$\phi_+^{(2)} = \sum_{n=1}^{\infty} C_n^+ e^{(2n-1)w_+} - i D_n^+ e^{2nw_+}, \tag{46}$$

and inside the lower (right-hand) cylinder,

$$\phi_-^{(2)} = \sum_{n=1}^{\infty} (C_n^- - i D_n^-) e^{-2anw_-} . \tag{47}$$

The matching procedure will occur as before with successive matching of ϕ [Eq. (45)] and $\partial\phi/\partial n$ first along the upper cylinder boundary (with $\phi_+^{(2)}$) and then along the lower cylinder boundaries (with $\phi_-^{(2)}$). Due to the asymmetry of the cylinder arrangement across the horizontal, the neat correspondence between upper and lower coefficients seen in the rectangular case will not appear in this triangular arrangement.

For the boundary conditions on the upper cylinder we write everything in terms of the upper frame variable, namely w_+. The applied potential, written in terms of w_+ from Eq. (41), is, to within a constant, just

$$\phi^{(\mathrm{app})}=e^{w_+}. \tag{48}$$

We now expand the hyperbolic functions (44) in terms of the eigenfunction (48). We have from Eqs. (41) and (42) that

$$e^{2anw_-}=\sigma^n\left(\frac{1-s/\sigma}{1-s}\right)^n, \tag{49}$$

where

$$s=\frac{e^{w_+}}{a-ib}, \quad \sigma=-\frac{a+ib}{a-ib}. \tag{50}$$

Since $|\sigma|=1$ and on the upper unit cylinder $|e^{w_+}|=1$ the use of the expansion (26) will be permissible whenever $a^2+b^2\geqslant 1$. For nonintersecting cylinders $a^2+b^2\geqslant 3$ and so the expansion of Eq. (49) using Eq. (26) is always possible on the upper cylinder.

Using Eq. (26) to expand Eq. (49) thus leads to

$$e^{\pm 2anw_-}=\sum_{k=0}^{\infty} P_{n,k}^{\pm}(a,b)e^{kw_+}, \tag{51}$$

where

$$P_{n,k}^{\pm}(a,b)=\pm\frac{2an}{a+ib}\,\frac{\sigma^{\pm n}}{(a-ib)^k}\,F_{2,1}\left(1-k,1\mp n;2;\frac{2a}{a+ib}\right). \tag{52}$$

Hence we obtain the hyperbolic functions in w_- in terms of the eigenfunctions e^{kw_+}:

$$\left\{\begin{matrix}\sinh 2anw_-\\ \cosh 2anw_-\end{matrix}\right\}=\sum_{k=0}^{\infty} Q_{n,k}^{\pm}e^{kw_+}, \tag{53}$$

where

$$Q_{n,k}^{\pm}=Q_{n,k}^{\pm}(a,b)=\tfrac{1}{2}[P_{n,k}^{+}(a,b)\pm P_{n,k}^{-}(a,b)]. \tag{54}$$

We now write down the boundary conditions (13) and (14) for the upper cylinder using Eqs. (43) and (46) for $\phi_+^{(1)}$ and $\phi_+^{(2)}$, Eqs. (44) and (53) for $\phi_-^{(1)}$, and Eq. (48) for $\phi^{(\mathrm{app})}$ and then eliminate C_k^+ and D_k^+. This generates two sets of equations: those in $\cos(2k-1)\theta$ and those in $\sin 2k\theta$. These turn out to be

$$\nu A_k^+-\sum_{n=1}^{\infty} Q_{n,2k-1}^{-,r}A_n^--\sum_{n=1}^{\infty} Q_{n,2k-1}^{+,i}B_n^-=\delta_{k,1}, \tag{55}$$

$$\nu B_k^+-\sum_{n=1}^{\infty} Q_{n,2k}^{-,i}A_n^--\sum_{n=1}^{\infty} Q_{n,2k}^{+,r}B_n^-=0, \tag{56}$$

where the superscripts r and i denote the real and imaginary parts, respectively.

We now match the outer potential ϕ [Eq. (45)] (and its normal derivative), with $\phi_-^{(2)}$ across the boundaries of the lower two cylinders. In this case everything is to be expressed in terms of the eigenfunctions appropriate to the lower cylinder pair. These are the functions e^{-2akw_-}. In particular, this must also be done for the applied potential which is again just Eq. (23) with w_- in place of w. We also use Eqs. (41) and (42) to express the exponentials in w_+ in terms of those in w_- and obtain

$$e^{-nw_+}=\frac{1}{(a-ib)^n}\left(\frac{1-s/\sigma}{1-s}\right)^n, \quad s=\sigma e^{-2aw_-}. \tag{57}$$

The convergent expansion of Eq. (57) along the lower right-hand cylinder using Eq. (26) is assured since on this boundary $u<0$ and so $|s|<1$. Hence, using Eqs. (26) and (57) we find that

$$e^{-nw_+}=\sum_{k=0}^{\infty} R_{n,k}(a,b)e^{-2akw_-}, \tag{58}$$

where

$$R_{n,k}(a,b)=\frac{2an}{a+ib}\,\frac{\sigma^k}{(a-ib)^n}\,F_{2,1}\left(1-k,1-n;2;\frac{2a}{a+ib}\right). \tag{59}$$

We now apply the boundary conditions (13) and (14) on the lower cylinder pair using Eqs. (44) and (47) for $\phi_-^{(1)}$ and $\phi_-^{(2)}$, Eqs. (43) and (58) for $\phi_+^{(1)}$, and Eq. (23) (in w_-) for $\phi^{(\mathrm{app})}$ and then eliminate the coefficients C_k^- and D_k^-. After separating coefficients of $\cos 2akv$ and $\sin 2akv$ in the result we obtain the following equations:

$$(\nu+\mu^k)A_k^--\sum_{n=1}^{\infty}\tilde{R}_{n,k}^{e,i}B_n^+-\sum_{n=1}^{\infty}\tilde{R}_{n,k}^{o,r}A_n^+=2a\mu^k, \tag{60}$$

$$(\nu+\mu^k)B_k^--\sum_{n=1}^{\infty}\tilde{R}_{n,k}^{o,i}A_n^++\sum_{n=1}^{\infty}\tilde{R}_{n,k}^{e,r}B_n^+=0, \tag{61}$$

where again the superscripts r and i denote real and imaginary parts, respectively, and

$$\tilde{R}_{n,k}^{\{{}_o^e\}}=\mu^k R_{\{{}_{2n-1}^{2n}\},k}. \tag{62}$$

The set (55), (56), (60), and (61) is now expressed in the (truncated) form (4):

$$(\nu\boldsymbol{I}_{4m}+\boldsymbol{S}_m^{(\mathrm{tri})})\cdot\mathbf{X}_m=\mathbf{Y}_m, \tag{63}$$

where

$$\mathbf{X}_m=\begin{pmatrix}\mathbf{A}_m^+\\ \cdots\\ \mathbf{B}_m^+\\ \cdots\\ \mathbf{A}_m^-\\ \cdots\\ \mathbf{B}_m^-\end{pmatrix},\quad \mathbf{Y}_m=\begin{pmatrix}\mathbf{D}_m\\ \cdots\\ \mathbf{O}_m\\ \cdots\\ \mathbf{K}_m\\ \cdots\\ \mathbf{O}_m\end{pmatrix}, \tag{64}$$

and with a structure matrix

$$\boldsymbol{S}_m^{(\mathrm{tri})}=\left(\begin{array}{ccc:c:cc}
 & \boldsymbol{O}_{2m} & & \vdots & -\boldsymbol{Q}_m^{-,r} & -\boldsymbol{Q}_m^{+,i}\\
 & & & \vdots & \cdots & \cdots\\
\cdots & \cdots & \cdots & \vdots & -\boldsymbol{Q}_m^{-,i} & \boldsymbol{Q}_m^{+,r}\\
-\tilde{\boldsymbol{R}}_m^{o,r} & \vdots & -\tilde{\boldsymbol{R}}_m^{e,i} & \vdots & \cdots & \cdots\\
\cdots & \vdots & \cdots & \vdots & \boldsymbol{E}_m & \boldsymbol{O}_m\\
-\tilde{\boldsymbol{R}}_m^{o,i} & \vdots & \tilde{\boldsymbol{R}}_m^{e,r} & \vdots & \cdots & \cdots\\
 & & & \vdots & \boldsymbol{O}_m & \boldsymbol{E}_m
\end{array}\right), \tag{65}$$

where the $\mathbf{A}_m^{\pm}$ and $\mathbf{B}_m^{\pm}$ denote the vectors of coefficients $A_i^{\pm}$ and $B_i^{\pm}$, respectively, the $\tilde{\boldsymbol{R}}_m^{p,q}$ and the $\boldsymbol{Q}_m^{\pm,q}$ $(p=o,e;\ q=r,i)$ are matrices of elements $\tilde{R}_{i,j}^{p,q}$ and $Q_{i,j}^{\pm,q}$, respectively, and $\mathbf{D}_m$ is the column vector with elements δ_{1j}.

In this case the overall polarization will be the sum of the contributions of the upper cylinder (the A_1^+ term) and of the lower cylinder pair (the A_n^- terms). Hence for the triangular cluster we obtain

$$\langle\chi\rangle_{\mathrm{tri}}=\frac{2}{3}\left(A_1^+ +4a\sum_{n=1}^{m} nA_n^-\right) \tag{66}$$

which leads to the spectral representation (1) in which

$$g_n=\frac{2}{3}\left(u_{1n}+4a\sum_{k=1}^{m} ku_{2m+k,n}\right)\left(\overline{u}_{n1}+2a\sum_{k=1}^{2m}\mu^k\overline{u}_{n,2m+k}\right),$$

$$L_n=\tfrac{1}{2}(1-t_n), \tag{67}$$

where, again, the u_{ij} and $\overline{u_{ij}}$ are the elements of the matrices that diagonalize the structure matrix $\boldsymbol{S}_m^{(\mathrm{tri})}$ and the t_n are the eigenvalues of this matrix.

V. APPLICATION OF THE TECHNIQUE

Interest in effective medium theory is currently being motivated by the desire to understand the optical behavior of composite thin films [16,17]. Of particular interest in this regard are films formed by the deposition of metallic inclusions into a columnar dielectric matrix. The Maxwell-Garnett and Bruggeman formulations still dominate when it comes to interpretation of experimental data for such composites. Lately, for example, inversion of spectroscopic ellipsometric data with these simple models has been used to obtain fill factors for voids in thin coatings [18]. In such interpretive work, knowledge of the detailed make-up of observed absorption peaks in the overall response is crucial in determining geometric parameters. What appears as an individual resonance may in fact be the accumulated superposition of several of these. The unfounded (and often false) assumptions of this type, which then arise, are bound to produce suspect values for the sought-after structural constants.

The problem theoretically has of course been to develop expressions for effective dielectric responses as functions of the given geometry within which are also differentiated all the individual resonances. The merit of the work done in the preceding sections is that such a method for finite clusters has been developed and successfully applied to rectangular and triangular cylinder arrangements. It is a simple matter (see Sec. VI) to show that the technique is applicable to any arrangement at all that consists of a finite number of nonintersecting circular cylinders. However, an examination of the numerous experimental implications thrown up by this more general scenario merits a separate study. Here we shall restrict ourselves to predictions made by the formulas of Secs. III and IV for the rectangular and triangular clusters. In particular we shall consider the case of aluminum cylinders in air and focus on the distribution of resonances producing the absorption profiles.

We begin with two special cases, the square arrangement of four cylinders and the equilateral triangular arrangement of three cylinders. Plots of the imaginary part of the polarizability using Eqs. (39) and (40) and Eqs. (66) and (67) have been determined and are both shown in Fig. 4, each for two different intercylinder spacings. In both cases the single isolated cylinder response is included for comparison. The overall similarity in the responses of the two arrangements is striking. An examination of the first few individual resonances for the case $b=d=1.1$ in the square is shown in Fig. 5(a) and for the analogous case ($l=2.2$, $\varphi=\pi/6$) in the equilateral triangle in Fig. 5(b). Few of the corresponding absorption peaks discernible in Fig. 4 in this close-approach case represent the contribution of only a single resonance. The overlap between individual resonances is particularly marked

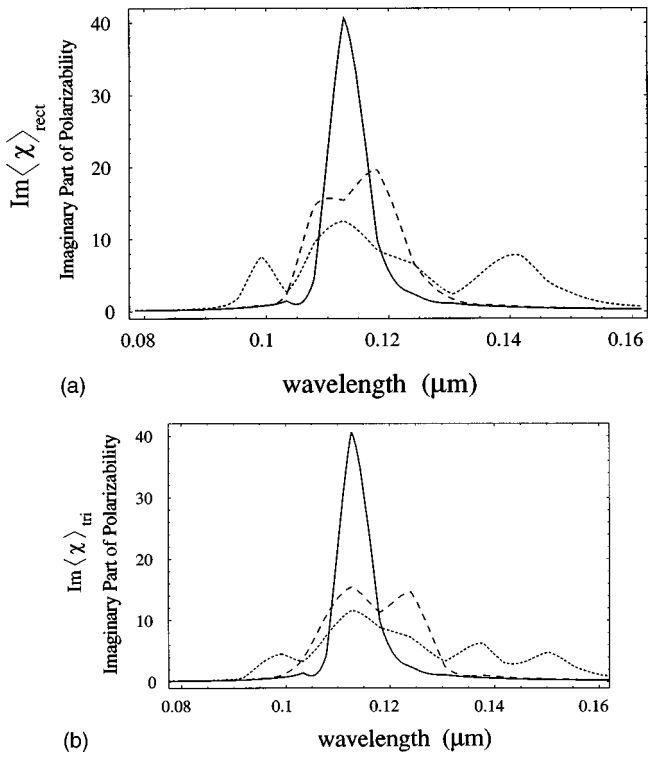

FIG. 4. (a) The imaginary part of the polarizability for a square cluster ($b=d$) of aluminum cylinders in air. Response curves as a function of wavelength λ are shown for the case $d=1.1$ (dotted), $d=1.5$ (dashed), and $d=\infty$ (solid). (b) The imaginary part of the polarizability for equilateral triangular clusters of unit circular cylinders ($b=\sqrt{3}d$). Response curves as a function of wavelength λ are shown for $d=1.1$ (dotted), $d=1.5$ (dashed), and $d=\infty$ (solid). The cases $d=\infty$ correspond to a single isolated cylinder.

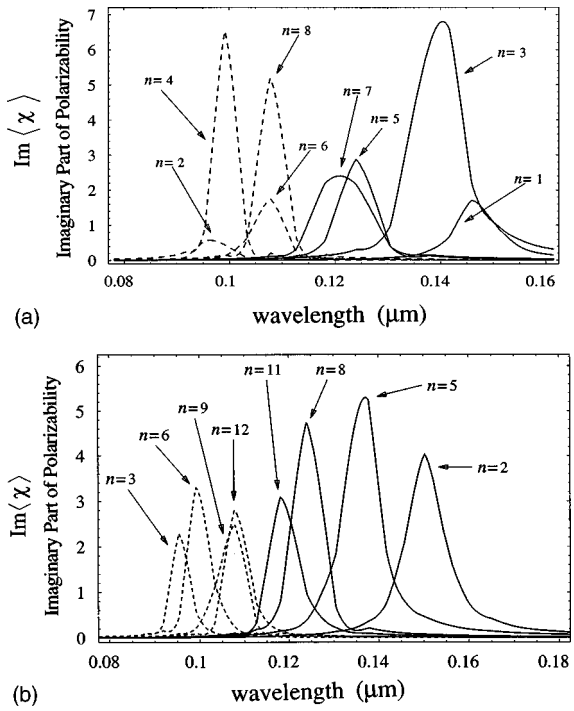

FIG. 5. The resonant structures for (a) the square and (b) the equilateral triangular clusters in the case $d=1.1$. Individual plots corresponding to the first four eigenvalue sets (displayed in Tables I and II) are shown. Resonances corresponding to the positive (solid) and negative (dashed) eigenvalues t_n are shown.

in the rectangular cluster, although for the equilateral triangle there is relatively little of this overlap between the first couple of resonances. Further investigation revealed that this overlapping phenomenon continued to manifest itself in the case of the remaining peaks apparent in Fig. 4 for this particular intercylinder spacing. This, however, is to be expected since as n increases both the eigenvalues t_n and the spectral weights g_n approach zero. There will thus always be an accumulation of successively less intense resonances closer and closer to $\epsilon'=-1$. In other words the higher order resonances accumulate at a wavelength λ_c satisfying $\epsilon'(\lambda_c)=-1$. We also note that the small sharp peak appearing near $\lambda=0.1$ μm in the responses of the isolated cylinders is not a resonance but merely an artifact of the optical constant. Its effect disappears completely in the presence of the cluster interactions.

The interesting aspect of the square and equilateral geometries of Figs. 4 and 5 is that both longitudinal and transverse responses will be the same. For the equilateral triangle a simple geometric argument suffices to demonstrate this. A useful check on our results can be deduced from this observation. We first consider the general response function in its form (10) and note that by Keller's theorem the orthogonal response is obtained by merely replacing ν with $-\nu$. In other words the orthogonal result is obtained just by replacing the original set of eigenvalues by their negative counterparts. Therefore, for both the square and equilateral triangular arrangements the respective eigenvalue sets must be invariant under sign change. This can only be the case if the eigenvalues appear in positive-negative pairs of the form $\{t_k,-t_k\}$. Moreover the eigenvalues in each pair will share a common spectral weight g_k. Tables I and II show the first few eigenvalues and spectral weights corresponding to the resonances shown in Fig. 5 [the square ($b=d=1.1$) and equilateral triangle ($l=2.2$, $\varphi=\pi/6$)]. As we see in Table I, the expected pattern in the eigenvalues for the square cluster does indeed appear. The expected pattern of eigenvalues also appears in Table II for the triangular cluster, but in an unexpected way. Here the eigenvalues actually appear in triplets of the form $\{t_k'',t_k',-t_k'\}$. The members of the positive-negative pair $\pm t_k'$ share the same weight g_k' while the weight of the ''odd one

TABLE I. The first four sets of eigenvalue pairs for the square cylinder cluster with $b=d=1.1$. Also shown are the corresponding spectral weights, g_n, and the depolarization factors, L_n.

n	t_n	g_n	L_n
1	0.405 390	0.029 665	0.297 305
2	−0.405 390	0.029 665	0.702 695
3	0.345 673	0.142 873	0.327 163
4	−0.345 673	0.142 874	0.672 836
5	0.155 120	0.056 157	0.422 440
6	−0.155 106	0.056 180	0.577 553
7	0.121 042	0.096 354	0.439 479
8	−0.121 008	0.096 452	0.560 504

TABLE II. The first four sets of eigenvalue triplets for the equilateral triangular cylinder cluster with $l=2.2$ and $\phi=\pi/6$. Also shown are the corresponding spectral weights, g_n, and the depolarization factors, L_n.

n	t_n	g_n	L_n
1	0.648 844	0.000 000	0.175 578
2	0.434 769	0.069 010	0.282 615
3	−0.434 769	0.069 011	0.717 384
4	0.329 847	0.000 000	0.335 077
5	0.307 517	0.117 074	0.346 242
6	−0.307 514	0.117 075	0.653 757
7	0.185 782	0.000 000	0.407 109
8	0.158 878	0.088 783	0.420 561
9	−0.158 877	0.088 783	0.579 438
10	0.103 340	0.000 000	0.448 330
11	0.098 597	0.075 077	0.450 702
12	−0.098 595	0.075 077	0.549 298

out,'' t_k'', is precisely zero. Hence the equivalence in the response for both directions is also guaranteed for the equilateral triangular cluster.

A useful check on the correctness and degree of accuracy of the method is the satisfaction of the sum rule (3) for the spectral weights g_n. In every case considered this sum rule was satisfied once the truncation order had become sufficiently large. In fact, the nearness of the total sum to unity acts as a useful measure of the accuracy achieved for a given truncation order.

Another way of gaining some insight into the relationship between geometric arrangement and resonant distribution is to consider triangular clusters with differing internal angles. In Fig. 6 we plot the absorption profiles for three different triangular geometries. In each case $l=2.2$. We consider a collinear arrangement ($\varphi=\pi/2$) and two others ($\varphi=\pi/3$, $\varphi=\pi/6$). The last one is the equilateral case treated earlier. It is included here for the sake of comparison. Detailed inspection of the resonant structure of the two noncollinear cases again reveals that the absorption peaks in these cases result from multiple overlapping of individual resonances. However, in the collinear geometry, the observed peak at $\lambda=0.155\ \mu$m is effectively the single resonance corresponding to the first positive eigenvalue. The first four resonances with non-negligible weights for this collinear arrangement are plotted in Fig. 7.

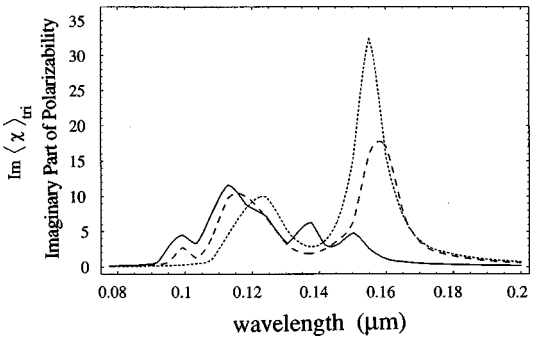

FIG. 6. Response curves for three different triangular arrangements of aluminum cylinders in air. The imaginary part of the polarizability as a function of wavelength λ is plotted for $l=2.2$ and $\varphi=\pi/2$ (collinear arrangement, shown dotted), $\varphi=\pi/3$ (shown dashed), and $\varphi=\pi/6$ (equilateral arrangement, shown solid).

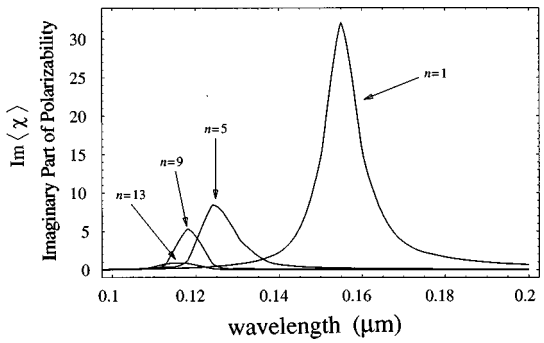

FIG. 7. Resonances corresponding to those positive eigenvalues t_n with the four greatest weights g_n for the collinear arrangement ($l=2.2$, $\varphi=\pi/2$) of three aluminum cylinders in air.

Unlike the square and (nondegenerate) triangular arrangements, the collinear case shown in Figs. 6 and 7 exhibits an isolated first or fundamental polarization mode. It is interesting to note that this type of response is also observed for the case of two cylinders [10] and for an infinite chain of metal cylinders [11]. It would seem that collinear or chainlike arrangements tend to produce this type of behavior. This has obvious significance when the simple dipole models are used to fit such curves.

VI. SOLUTION FOR A GENERAL CLUSTER

It is now quite a simple matter to show that the foregoing superposition technique can be used for any finite cluster of identical nonintersecting cylinders. The sum of any finite number of harmonic functions that vanish at infinity is again a harmonic function vanishing at infinity and so all we need to show is that the relevant convergence requirements will always be met. We shall first consider a completely general finite cluster with no exploitable symmetries and then move on to a consideration of those with at least one axis of symmetry.

For a cluster admitting no symmetry axes we simply consider each individual cylinder as a subcluster and assign the appropriately centered polar frame to each one. Hence for such a cluster consisting of n cylinders we will have n polar frames and consequently an outer potential that is the sum of the n local outer potentials. Checking the convergence requirement between any two polar frames is straightforward. Consider then two unit cylinders [(1) and (2), say] centered at the points $z=0$ and $z=\alpha$ with local frames $w_1=\ln z$ and $w_2=\ln(z-\alpha)$, respectively. The outer potential in the local frame w_1 for cylinder (1) will be a series in powers of e^{-w_1} and the eigenfunctions for cylinder (2) will be the functions e^{kw_2}. Hence we consider

$$e^{-nw_1}=z^{-n}=\alpha^{-n}\left(1+\frac{e^{w_2}}{\alpha}\right)^{-n}. \tag{68}$$

For nonintersecting cylinders $|\alpha|\geqslant 2$. Moreover, $|e^{w_2}|=1$ on the boundary of cylinder (2) and so we can expand the bino-

mial in Eq. (68) in a convergent series in positive powers of e^{w_2} along this boundary. The convergence criteria between arbitrary polar coordinate frames are thus met and so the superposition technique will work in this completely general case.

We now briefly consider cylinder arrangements that admit *at least* one symmetry axis. The advantage here is that we can usually make use of the symmetries in order to reduce the number of coordinate frames used. This leads to a corresponding reduction in the number of coefficient sets and thus also in the matrix sizes. This is exemplified in the case of the rectangular cluster of Sec. III. We consider an orientation in which the chosen symmetry axis is vertical and note that the individual cylinders in the cluster will either (i) lie centered on the given symmetry axis, or (ii) lie in image pairs to the left and right of this axis. We then proceed as follows. To each cylinder in category (i) we assign the appropriately centered polar coordinate frame and write inner and outer local potentials in terms of these polar coordinates. For the cylinder pairs in category (ii) we operate similarly with the appropriately positioned bicylindrical coordinates. Hence all the frames will share a common central axis. The total induced potential outside the cluster will be the sum of the local outer potentials. The matrix equation (4) for all the outer coefficients is then obtained by successively matching this sum on each single cylinder and cylinder pair one after the other and then eliminating all inner coefficients. For each matching all eigenfunction expansions are reexpressed in terms of the local variables for a given boundary contour. All we need to do is show that these expansions of the eigenfunctions are always convergent on the given cylinder boundary. These expansions will occur between either (a) one bicylindrical frame and another and/or (b) a bicylindrical frame and a polar frame and/or (c) one polar frame and another. The solution obtained in Sec. III shows that case (a) is possible when both bicylindrical frames have the same pole positions. In Appendix A we show that the convergence criteria are also satisfied between two bicylindrical frames having different pole positions. Hence case (a) is always solvable. The solution obtained in Sec. IV for the triangular cluster immediately disposes of case (b) and for case (c) the required convergence property between two polar frames has been demonstrated in the preceding paragraph. A superposition of bicylindrical and polar coordinate frames can thus always be used to find the quasistatic response for cylinder clusters with the above-mentioned symmetry property.

VII. CONCLUSION

We have shown that a superposition technique employing combinations of polar and/or bicylindrical coordinate frames can provide an explicit normal-mode representation for the response of any finite cluster of identical nonintersecting cylinders. The method leads quite naturally to the Bergman decomposition. Moreover, there are no restrictions on the dielectric constants of the two phases nor on the proximity of cylinders to each other. The major strength of the approach is that the detailed resonant structure of any response can be readily probed. In particular, we have unearthed evidence to suggest that in most clusters one can expect many of the absorption peaks to be the result of aggregates of overlapping resonances. The exception seems to be for some triangular structures and for chainlike structures when the field acts along the chain axis. In these instances the fundamental mode (the $n=1$ resonance) may often remain more or less isolated from all the higher-order modes. Further study of more extensive chains and rectangular clusters with this approach may confirm these tentative conclusions for larger and more general clusters. Concurrent work in this direction is being pursued and should appear in forthcoming publications.

ACKNOWLEDGMENTS

This work was undertaken while one of the authors (A.J.R.) was supported by an Australian Research Council (ARC) grant. The authors would like to thank their colleagues Ross McPhedran, Nicolae Nicorovici, and Lindsay Botten at the University of Sydney's Department of Theoretical Physics for several helpful discussions. Thanks are also due to Phillip Abbot for his help with the figures.

APPENDIX A

In the general arrangement of four unit cylinders with one axis of symmetry, we consider two bicylindrical coordinate frames, w_+ and w_-, for the upper and lower pairs, respectively. If the corresponding pole positions are denoted $a_\pm$, then the respective cylinder centers will be denoted $(\pm d^+, b)$ and $(\pm d_-, -b)$, where

$$d_\pm = \sqrt{1+a_\pm^2}. \tag{A1}$$

We thus have

$$w_\pm = \frac{1}{2a_\pm} \ln\left(\frac{z+a_\pm - ib}{z-a_\pm - ib}\right). \tag{A2}$$

Suppose we are expanding the local potential expansion for the lower pair around the upper right-hand cylinder. We must then expand exponentials in w_- in terms of exponentials in w_+. We need only do one case. For instance,

$$e^{2a_- n w_-} = \left(\frac{z+a_- + ib}{z-a_- + ib}\right)^n \tag{A3}$$

$$= \varrho^n \left(\frac{1-\zeta/\varrho^2}{1-\zeta}\right)^n, \tag{A4}$$

where

$$\varrho = \frac{a_+ + a_- + 2ib}{a_+ - a_- + 2ib} \tag{A5}$$

and

$$\zeta = \varrho e^{-2a_+ w_+}. \tag{A6}$$

Along the upper right-hand cylinder we have

$$\left|e^{-2a_+ u_+}\right| = e^{-2a_+ u_+} = \frac{1}{a_+ + \sqrt{1+a_+^2}}. \tag{A7}$$

Convergence will thus be guaranteed when

$$|\zeta_1| = \varrho e^{-2a_+ u_+} = \frac{1}{a_+ + \sqrt{1+a_+^2}} \left(\frac{(a_+ + a_-)^2 + 4b^2}{(a_+ - a_-)^2 + 4b^2} \right)^{1/2} \leqslant 1. \tag{A8}$$

For nonintersecting cylinders we require the center-to-center distance between the right-hand cylinders to be greater than two units. This condition is

$$2\Delta = a_+^2 + a_-^2 + 2 - 2\sqrt{1+a_+^2}\sqrt{1+a_-^2} + 4b^2 \geqslant 0. \tag{A9}$$

The square of $|\zeta_1|$ can thus be rewritten

$$(1 + 2a_+^2 - 2a_+\sqrt{1+a_+^2}) \times \frac{\Delta + \sqrt{1+a_+^2}\sqrt{1+a_-^2} + 1 + a_+ a_-}{\Delta + \sqrt{1+a_+^2}\sqrt{1+a_-^2} + 1 - a_+ a_-}, \tag{A10}$$

which is a monotonically decreasing function of Δ for all positive a_+ and a_-. Hence its maximum value will occur on $\Delta = 0$. This is attained along $a_+ = 0$ and is precisely unity. Hence the necessary and sufficient condition for the superposition of arbitrary bicylindrical frames with a common axis of symmetry is assured.

[1] R. Landauer, in *Electrical Transport and Optical Properties of Inhomogeneous Media, Ohio State University, 1977*, edited by J. C. Garland and D. B. Tanner (American Institute of Physics, New York, 1978).

[2] J. C. M. Garnett, Philos. Trans. R. Soc. London, Ser. A **203**, 385 (1904); **205**, 237 (1906).

[3] H. A. Lorentz, *Theory of Electrons*, 2nd ed. (Teubner, Leipzig, 1916).

[4] L. Lorenz, Ann. Phys. (Leipzig) **11**, 70 (1880).

[5] R. Rojas and F. Claro, Phys. Rev. B **34**, 3730 (1986).

[6] R. Fuchs and F. Claro, Phys. Rev. B **39**, 3875 (1988).

[7] D. J. Bergman, Phys. Rep., Phys. Lett. **43C**, 377 (1978).

[8] A. V. Radchik, G. B. Smith, and A. J. Reuben, Phys. Rev. B **46**, 6115 (1992).

[9] A. J. Reuben, A. V. Radchik, and G. B. Smith, J. Phys. A **26**, 2021 (1993).

[10] A. J. Reuben, G. B. Smith, and A. V. Radchik, Ann. Phys. (N.Y.) **242**, 52 (1995).

[11] J. Kempe, A. V. Radchik, and G. B. Smith, Proc. R. Soc. London, Ser. A **452**, 1845 (1996).

[12] J. B. Keller, J. Math. Phys. **5**, 548 (1964).

[13] P. M. Morse and H. Feshbach, *Methods of Theoretical Physics*, Vol. 1 (Springer, New York, 1953).

[14] *Bateman Manuscript Project*, Vol. 3, edited by A. Erdelyi *et al.* (McGraw-Hill, New York, 1953).

[15] *Handbook of Mathematical Functions with Formulas, Graphs and Mathematical Tables*, edited by M. Abramowitz and I. A. Stegun (Dover, New York, 1972).

[16] R. J. Ditchburn and G. B. Smith, J. Appl. Phys. **69**, 3769 (1991).

[17] G. W. Mbise, D. Le Bellac, G. A. Niklasson, and C. G. Granqvist, J. Phys. D **30**, 1 (1997).

[18] K. Vedam and S. Y. Kim, Appl. Opt. **28**, 2691 (1989).